ORNL/LTR-2016/630

Comparison of Hybrid K-Edge Densitometer (HKED) Performance Operating with the Canberra Lynx MCA and the Canberra ICB-NIM electronics

Robert McElroy

October 2016

Approved for public release. Distribution is unlimited.

OAK RIDGE NATIONAL LABORATORY
MANAGED BY UT-BATTELLE FOR THE US DEPARTMENT OF ENERGY

DOCUMENT AVAILABILITY

Reports produced after January 1, 1996, are generally available free via US Department of Energy (DOE) SciTech Connect.

Website http://www.osti.gov/scitech/

Reports produced before January 1, 1996, may be purchased by members of the public from the following source:

National Technical Information Service
5285 Port Royal Road
Springfield, VA 22161
Telephone 703-605-6000 (1-800-553-6847)
TDD 703-487-4639
Fax 703-605-6900
E-mail info@ntis.gov
Website http://www.ntis.gov/help/ordermethods.aspx

Reports are available to DOE employees, DOE contractors, Energy Technology Data Exchange representatives, and International Nuclear Information System representatives from the following source:

Office of Scientific and Technical Information
PO Box 62
Oak Ridge, TN 37831
Telephone 865-576-8401
Fax 865-576-5728
E-mail reports@osti.gov
Website http://www.osti.gov/contact.html

Nuclear Security and Isotope Technology Division

COMPARISON OF HYBRID K-EDGE DENSITOMETER (HKED) PERFORMANCE OPERATING WITH THE CANBERRA LYNX MCA AND THE CANBERRA ICB-NIM ELECTRONICS

Robert McElroy

Date Published: October, 2016

Prepared by
OAK RIDGE NATIONAL LABORATORY
Oak Ridge, Tennessee 37831-6283
managed by
UT-BATTELLE, LLC
for the
US DEPARTMENT OF ENERGY
under contract DE-AC05-00OR22725

Comparison of Hybrid K-Edge Densitometer (HKED) Performance Operating with the Canberra Lynx MCA and the Canberra ICB-NIM Electronics

Robert D. McElroy, Oak Ridge National Laboratory

1. Introduction

From the 1991 until 2008 the Canberra Hybrid K-Edge Densitometer systems were provided with ICB-NIM (Integrated Control Bus – Nuclear Instrument Module) acquisition electronics. Newer electronics modules, such as the Lynx, were not supported under the VMS based operating system. The LYNX module was provided as the standard acquisition electronics following the release of the Windows based CHKED software. This report compares the electronics dead-time, gain shifts, detector resolution and measurement performance of the HKED system operated with the two types of acquisition modules. The comparison was performed using measurements obtained with the ORNL HKED system.

The original intent of this study was to take advantage of both the timing and energy outputs from the HPGE detector to acquire data with both sets of electronics in parallel. Although this approach has been applied successfully with other systems, in this case we found the timing output produced a significant amount of noise such that a comparison between the electronics would be invalid. So the comparative measurements were performed sequentially. The ICB-NIM data was acquired over the course of 12 months with 255 measurements while the LYNX data was acquired over a period of 10 months with 75 measurements.

To simplify the comparison, all data used in this study was acquired using the Canberra CHKED (V1.0) software package. The performance analysis was based primarily on the peak locations, peak widths and concentration values reported by the CHKED software. The raw spectra from the XRF measurements were also examined to extract additional ^{109}Cd peak location and width data for the hybrid measurements (the standard hybrid report template does not report these values).

1.1. ICB-NIM Components

The acquisition electronics and HPGe detectors used with the ICB-NIM based HKED measurements are provided in Table 1. The XRF and KED acquisition electronics chains each consist of an HVPS module, two point gain stabilizer, analog amplifier and ADC. A Remote Parallel Interface (RPI) module monitors the sample position switch to indicate proper sample loading. A single Ethernet Acquisition Interface Module (AIM) controls these modules and provides the interface to the host computer. A photograph of the HKED NIM bin with the ICB-NIM electronics is shown in Figure 1.

Table 1. HKED Detectors and ICB-NIM Electronics used with ORNL HKED system.

Qty	Model	Description
2	9645	ICB 6 KV HIGH VOLTAGE POWER SUPPLY
2	9615	ICB SPECTROSCOPY AMPLIFIER
2	9635	ICB 800 NSEC ADC, 8K CHANNEL
2	8233	TWO POINT DIGITAL STABILIZER
1	880777	554 Remote Parallel Interface
1	556A	Ethernet Acquisition Interface Module
1	2100-1	NIM BIN Power Supply 110VAC-150W
2 2 2 2	GL0210R 7600SL CC-HD C1551-30	Low Energy Germanium Detector SLIMLINE HORIZONTAL DIPSTICK Cryo cycle ALL-IN-ONE DETECTOR CABLE SET, 30 FT

Figure 1. ICB-NIM acquisition electronics rack for the ORNL HKED system.

1.2. LYNX Components

The acquisition electronics and HPGe detectors used with the LYNX based HKED measurements are provided in Table 1. The XRF and KED acquisition electronics chains each consist only of a LYNX module. The NIM bin, AIM and RPI modules were retained to provide a means to monitor the sample positioning sensor. However, although present, we were unsuccessful in our attempts to attach both the LYNX modules and the AIM module to the host computer through the CHKED software. Even though the AIM/RPI modules were not used in the LYNX measurements these modules were connected, so for completeness we have listed them here. A photograph of the LYNX modules is shown in Figure 2.

Table 2. HKED Detectors and Lynx used with ORNL HKED system.

Qty	Model	Description
2	LYNX	Lynx Digital Signal Processor
1	880777	554 Remote Parallel Interface
1	556A	Ethernet Acquisition Interface Module
1	2100-1	NIM BIN Power Supply 110VAC-150W
2	GL0210R	Low Energy Germanium Detector
2	7600SL	SLIMLINE HORIZONTAL DIPSTICK
2	CC-HD	Cryo cycle
2	C1551-30	ALL-IN-ONE DETECTOR CABLE SET, 30 FT

Figure 2. Photograph of the two LYNX modules that replace the ICB-NIM electronics rack. The two modules, side by side, are the same width but half the height of the NIM rack.

1.3. Measurement Configurations

The LYNX is a fully integrated Digital Signal Processing unit (DSP) that incorporates front end signal conditioning, a fast digitizing ADC, programmable digital filters, digital oscilloscope, automatic pole/zero and base line restorer, digital fast discriminator, two groups of 32K channel spectral memory, digital stabilizer and a triple-range HVPS. It replaces the NIM bin, HVPS, amplifier, ADC and interface control module typically used with the NIM based gamma-ray acquisition systems. The Lynx is operated through CANBERRA’s Genie 2000 software but may also be operated via the internet or a local area network (LAN). Based on the LYNX’s specifications; relative to the ICB-NIM, the LYNX should provide improved auto pole/zero and base line restoration capability. The signal filter function in principle requires less processing time, will be less sensitive to ballistic deficit, and is expected to provide superior resolution. This performance improvement was examined in this testing.

The ICB-NIM and LYNX data acquisition configurations are shown in Figure 3. For all measurements the ICB-NIM MCA used a shaping time of 1 μs while the LYNX DSP used settings of Rise Time = 2.8 μs and Flat top = 0.6 μs. High voltage, gain and other setting were adjusted to provide the proper peak locations for use with the CHKED software. Full listings of the settings for the ICB and LYNX modules for each detector are provided in Appendices A and B. The settings in the Appendices are taken from the Genie 2k Hardware report template for each configuration.

NOTE: There is some ambiguity since the CHKED software overrides the gain stabilization setting shown in Genie 2k printouts. The settings shown in Appendix A for the KED detector suggest that the gain stabilizer for the LYNX was turned off, however, the stabilizer was enabled for these measurements.

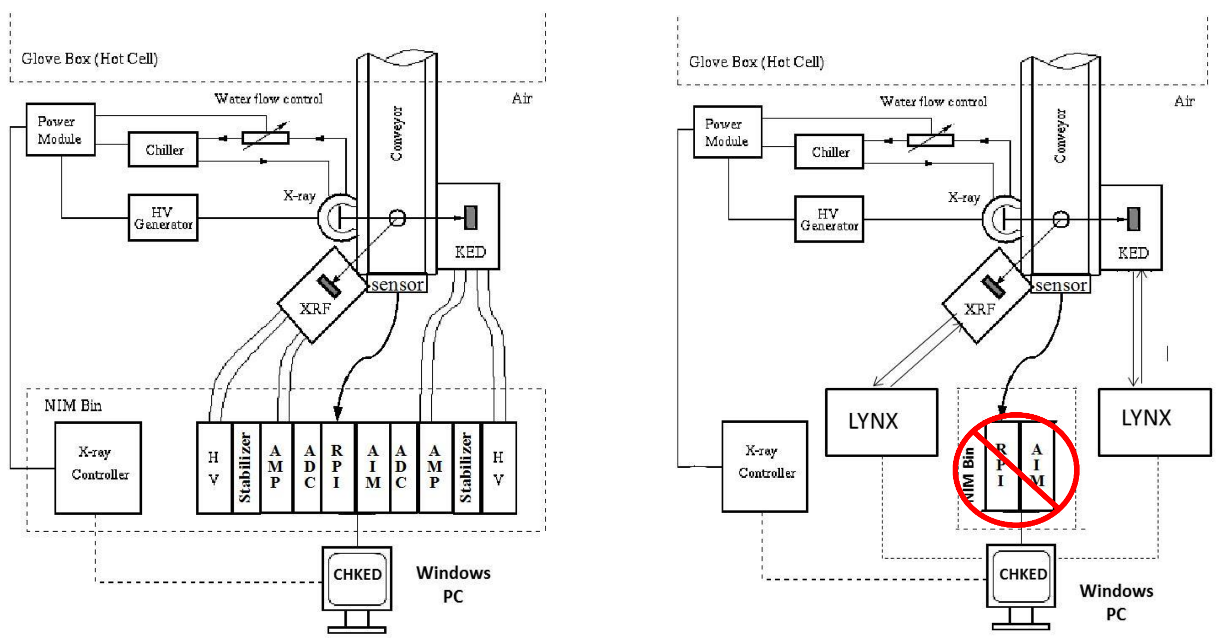

Figure 3. HKED system configurations for comparison measurements using the ICB-NIM (left) and Lynx modules (right). However, it was not possible to configure the CHKED software to operate with the LYNX modules and the RPI.

2. Electronic Dead-Time Effects

The dead-time as a function of count rate has been examined for both the KED and XRF for the ICB-NIM and LYNX based data acquisition systems (Figure 4 and Figure 5). The shape of the curve for each detector is unchanged by the change in electronics. The dead-time for the LYNX was found to be consistently lower than the NIM based electronics. For the XRF spectra the dead-time is 20% lower using the LYNX module, while for the KED spectra the dead-time is 25% lower. The obvious benefit to the improvement in dead-time is the shorter assay time required, however, there is also a reduction in the random coincidence summing effect. Figure 6 shows a comparison of spectra obtained using the ICB-NIM and LYNX modules for the same solution standard. The LYNX spectrum shows significantly lower coincidence summing than the ICB-NIM spectrum.

Note: the number of samples available during the LYNX testing was much smaller, however, each point seen on the curve below represents multiple assays.

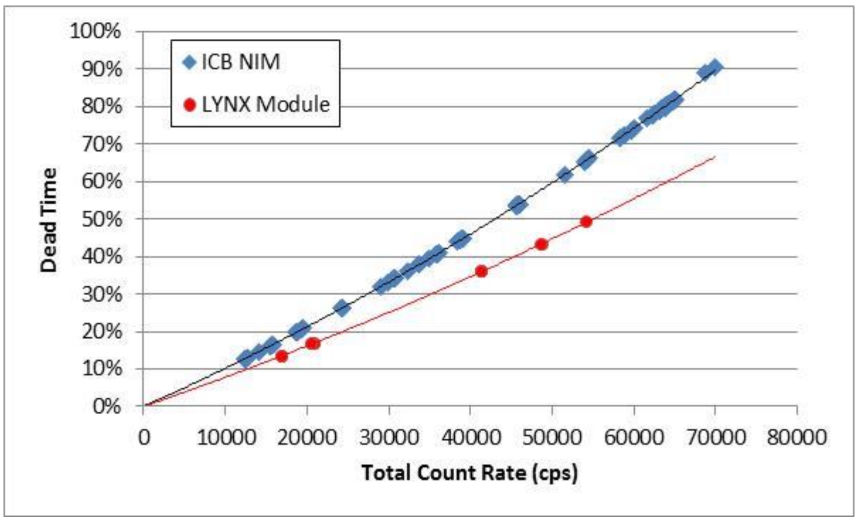

Figure 4. Dead-time as a function of count rate for the KED measurement.

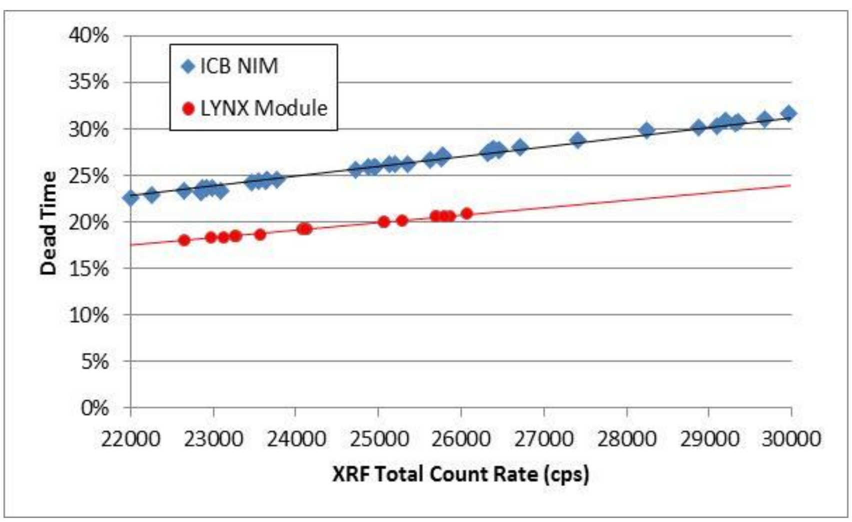

Figure 5. Dead-time as a function of count rate for the XRF measurement.

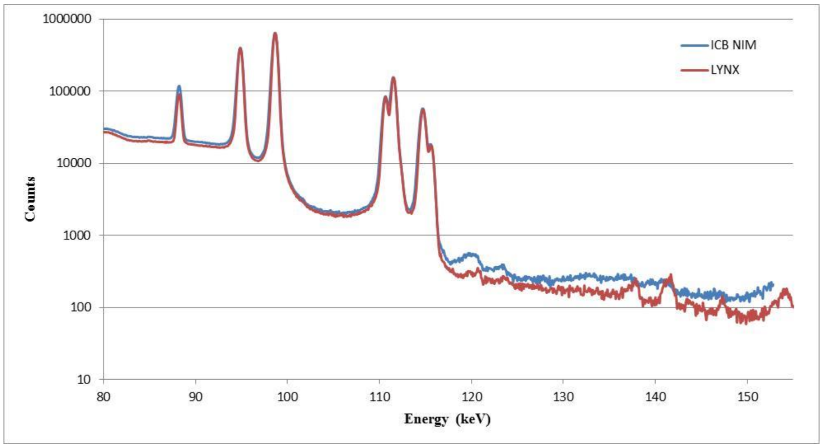

Figure 6. Overlay of the XRF spectra acquired for a 321 gU/L calibration standard using the ICB-NIM and LYNX modules illustrating the reduction in random coincidence summing with the LYNX module.

3. Stability

The stability/gain drift of the HKED system using the two different electronics configuration was examined using the reported peak locations from the CHKED software when available. The CHKED software provides the channel location of the Ag 22.1 keV X-ray and 88.034 keV gamma-ray from the decay of the ^{109}Cd reference source for the KED transmission spectrum. However, for the XRF spectrum the software reports only the peak centroid locations for the uranium and plutonium K-alpha lines. Additional analyses were performed on the raw XRF spectra to extract the peak location data for the 22.1 and 88.034 keV lines.

3.1. KED Detector Channel Stability

The CHKED software reports the channel location of the Ag 22.1 keV X-ray and 88.034 keV gamma-ray from the decay of the ^{109}Cd reference source. The results from hundreds of spectra were examined to determine the average peak location and standard deviation of the reported location (Table 3). Frequency distributions for the variation in the peak centroid for the 22.1 and 88 keV peaks are given in Figure 7 and Figure 8. We see that the ICB-NIM KED peak locations are slightly more stable than those obtained with the LYNX. For the 88 keV gamma-ray line from the ^{109}Cd reference source the difference amounts to approximately 0.2 channels or about 20 eV.

Table 3. KED Long Term Peak Stability and Centroid Location

Peak Energy (keV)	ICB NIM Electronics		LYNX Module	
	Centroid (channel)	Standard Deviation	Centroid (channel)	Standard Deviation
22.10	247.64	0.05	246.30	0.12
88.03	978.76	0.16	978.82	0.38
115.60	1284.50	0.24	1285.14	0.49
	Width (eV)	St. Dev.	Width (eV)	St. Dev.
FWHM ^{109}Cd 88 keV	512.6	7.9	507.9	12.7

Table 4 provides the average and extreme changes in the reference peak centroid channels and the U K-edge from the first repetition to the third. We see that the average grain drift over the course of an assay is again slightly smaller for the ICB NIM. For both acquisition systems, the average drift was small, <2eV for the ICB-NIM and <3eV for the LYNX module. By examination of the minimum and maximum shifts during an assay, we see that although the ICB-NIM provides a better average response, the extremes observed with the LYNX are smaller (10eV for the LYNX versus 30eV for the ICB-NIM. This suggests that the LYNX provides better stability in the short term (on the scale of an hour) but the ICB-NIM performs somewhat better over the course of weeks. In both cases the observed drifts within the assay are small and statistically insignificant.

Table 4. KED Gain Stability During Assay

	ICB NIM Electronics			**LYNX Module**		
Energy (keV)	22.1	88.03	115.6	22.1	88.03	115.6
Average Drift						
Δ Channels	-0.005	0.011	0.018	0.018	0.031	0.035
Δ keV	0.000	0.001	0.002	0.002	0.003	0.003
Maximum Negative Drift						
Δ Channels	-0.110	-0.110	-0.149	-0.040	-0.030	-0.057
Δ keV	-0.010	-0.010	-0.013	-0.004	-0.003	-0.005
Maximum Positive Drift						
Δ Channels	0.160	0.220	0.328	0.090	0.110	0.111
Δ keV	0.014	0.020	0.030	0.008	0.010	0.010

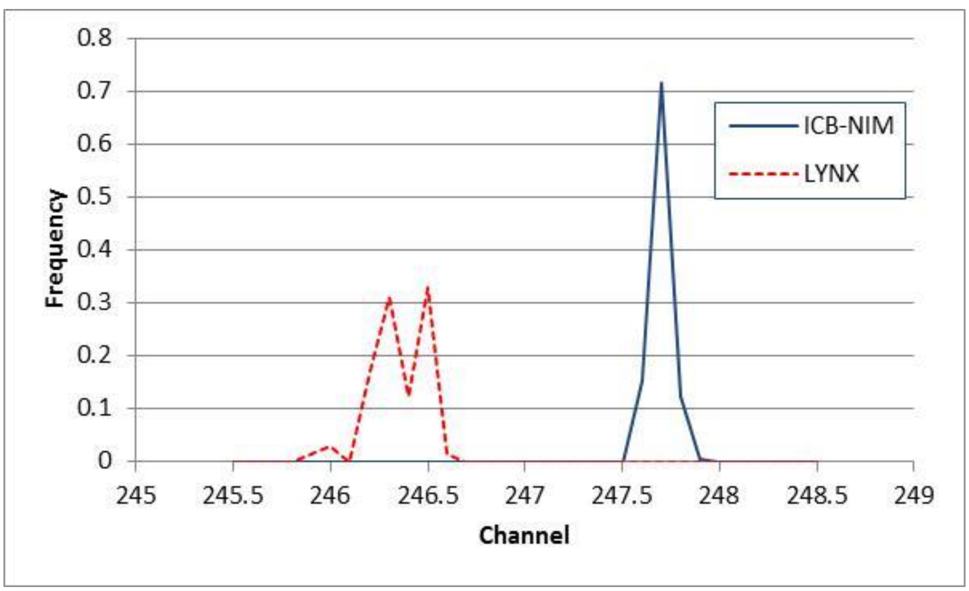

Figure 7. Frequency distribution for the observed 22.1 keV Ag X-ray peak location (from the decay of 109Cd) for the ICB-NIM and LYNX KED spectra.

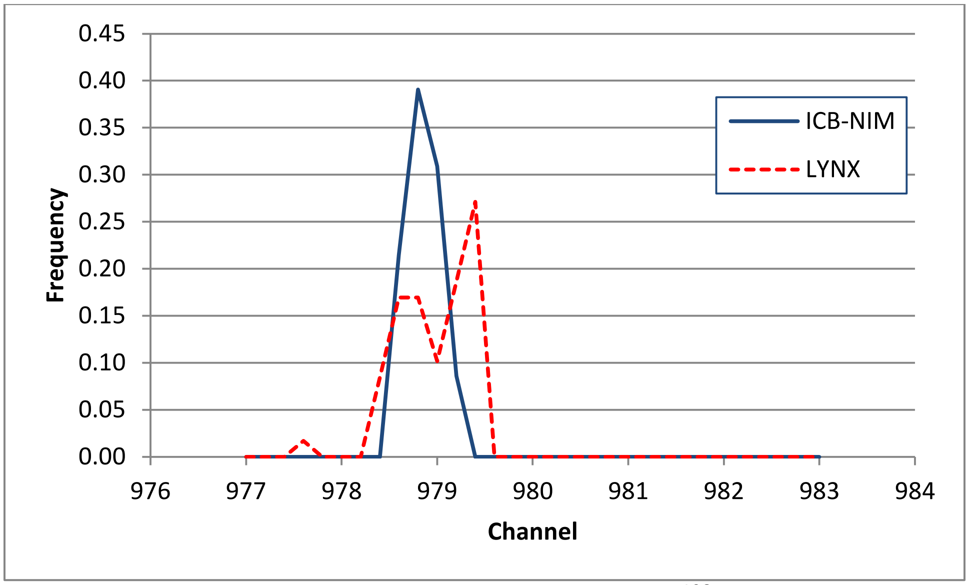

Figure 8. Frequency distribution for the observed ^{109}Cd 88.03 keVpeak location for the ICB-NIM and LYNX KED spectra.

3.2. KED Detector Channel Stability - Bias

Based on the 22.1 and 88.02 keV peak centroids, the CHKED software calculates an energy calibration and reports the channel number associated with the Uranium K-edge (115.6 keV). The K-edge ROIs are defined by the energy range about the K-edge and the corresponding channel numbers for the ROIs are determined using this energy calibration. The distribution in the calculated uranium K-edge channel number is shown in Figure 9. The width of the distribution is somewhat smaller for the ICB-NIM (0.24 vs 0.59 channels for the LYNX). Comparison of the reported concentration values shows equivalent measurement precision between the ICB-NIM and LYNX results.

Average bias in U concentration over the range of 100 g U/L to 321 g U/L.

- ICB-NIM: 0.6%
- LYNX: -0.5%

Average standard deviation over multiple assays 150 to 320 g U/L.

- ICB-NIM: 0.3%
- LYNX: 0.3%

The calibration biases are equivalent in magnitude although opposite in magnitude. The precision in the KED assay results is unaffected by the use of ICB-NIM or the LYNX.

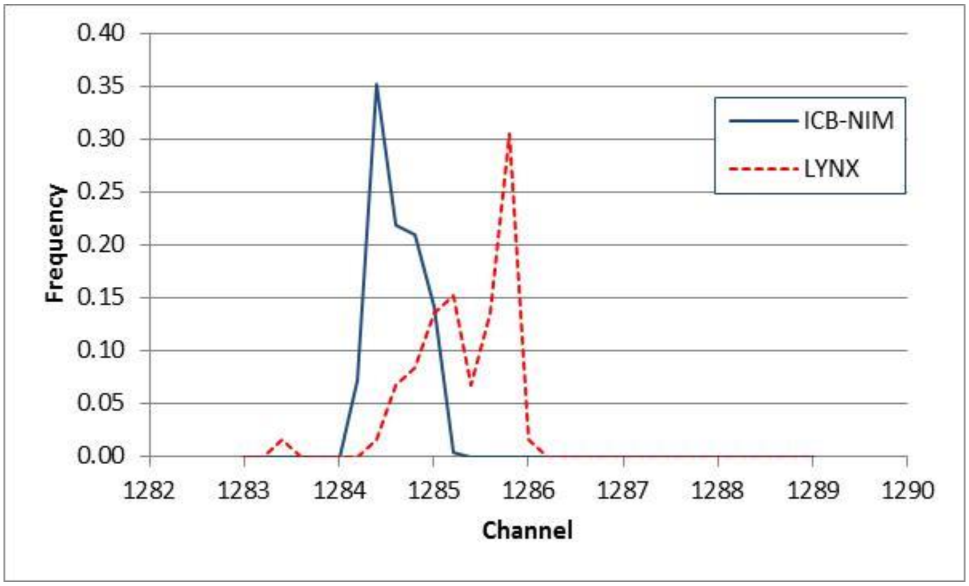

Figure 9. Frequency distribution for the reported K-edge location for the ICB-NIM and LYNX KED spectra.

3.3. XRF Detector Channel Stability

The CHKED software does not report the channel location of the Ag 22.1 keV X-ray and 88.034 keV gamma-ray from the decay of the ^{109}Cd reference source. The raw XRF spectra were examined to determine the average peak location and standard deviation of the reported location (Table 5). Frequency distributions for the variation in the peak centroid for the 22.1 and 88 keV peaks are given in Figure 10 and Figure 11. The peak location for the 88 keV line from the ^{109}Cd is more stable across the ICB-NIM spectra, however unlike the KED results, the spread in the 22.1 keV peak location is much narrower than for the ICB-NIM. The CHKED software provides the peak location and FWHM for the U Kα X-ray lines. These data were extracted from the report files and analyzed. Frequency distributions for the variation in the peak centroid for the 94.6 and 98.4 peaks are given in Figure 12 and Figure 13. A summary of the peak data is provided in Table 5. The LYNX module provides a small improvement in stability and energy resolution for the XRF detectors. This improvement is believed to be due the peak tail representing a smaller fraction of the peak area using the LYNX compared to the ICB-NIM.

The choice of acquisition electronics had no statistically significant effect on the assay results. However it is noted that the ICB-NIM measurement precision is on average 10% better (e.g. 0.065% vs 0.79%) than that observed for the LYNX data. This slight difference is attributed to the limited number of measurements available for this comparison.

Table 5. XRF Long Term Peak Stability and Centroid Location

Peak Energy (keV)	ICB NIM Electronics			LYNX Module		
	Centroid (channel)	Standard Deviation	FWHM (eV)	Centroid (channel)	Standard Deviation	FWHM (eV)
22.10	293.92	1.16		293.72	0.33	
88.03	1164.71	0.38		1164.02	0.28	
94.66	1251.22	0.47	577	1251.43	0.36	521
98.44	1301.22	0.49	588	1301.40	0.38	531

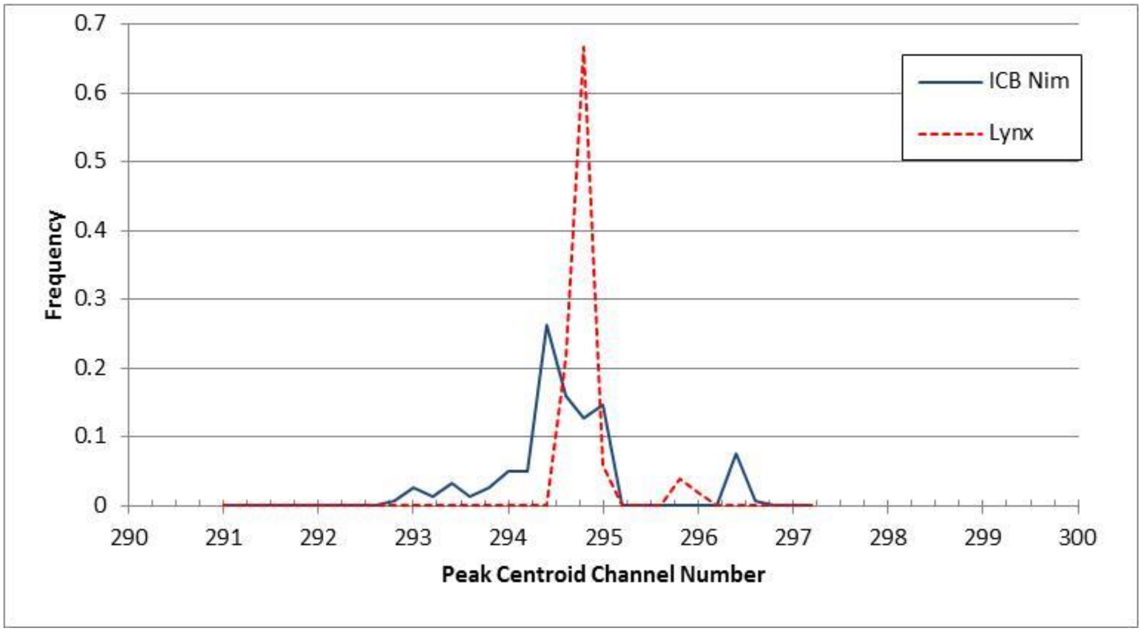

Figure 10. Frequency distribution for the observed 22.1 keV Ag X-ray peak location (from the decay of 109Cd) for the ICB-NIM and LYNX XRF spectra.

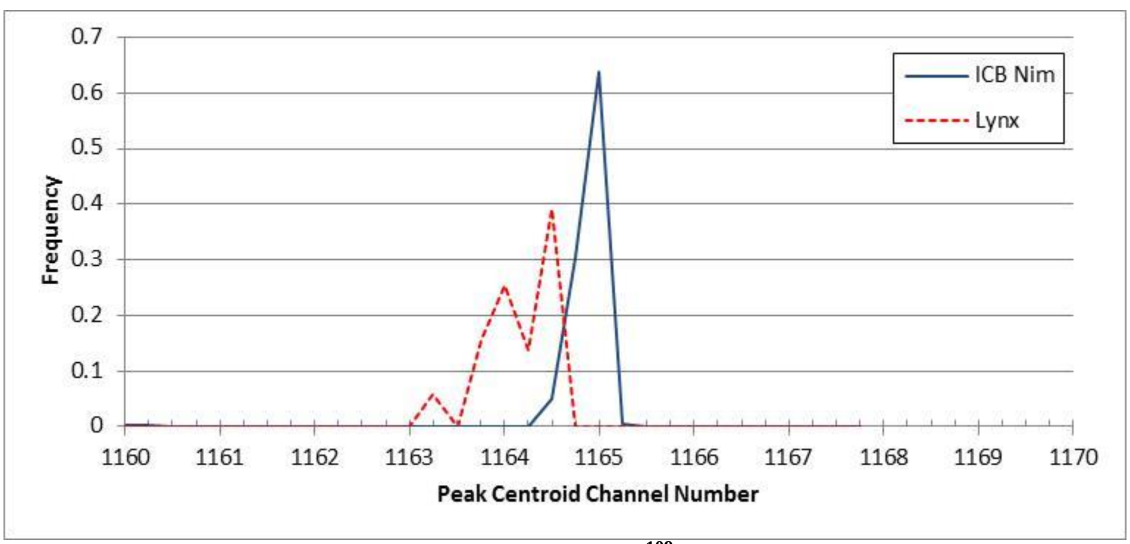

Figure 11. Frequency distribution for the observed ^{109}Cd 88.03 keVpeak location for the ICB-NIM and LYNX XRF spectra.

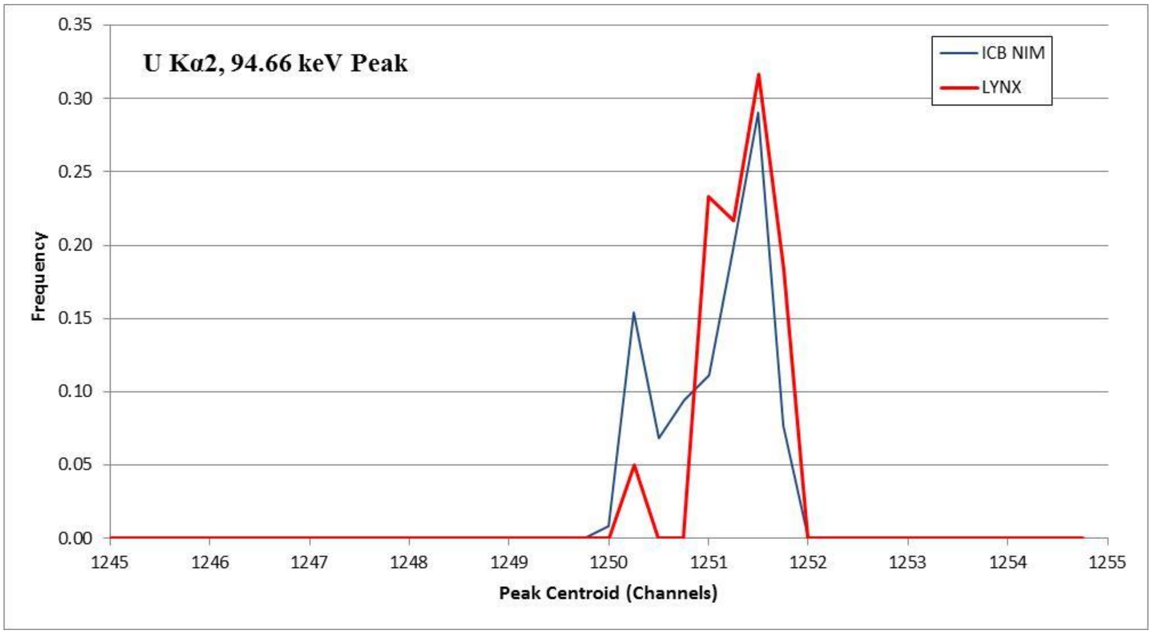

Figure 12. Frequency distribution for the observed 94.66 keV U $K_{\alpha 2}$ peak location for the ICB-NIM and LYNX XRF spectra as reported by the CHKED software.

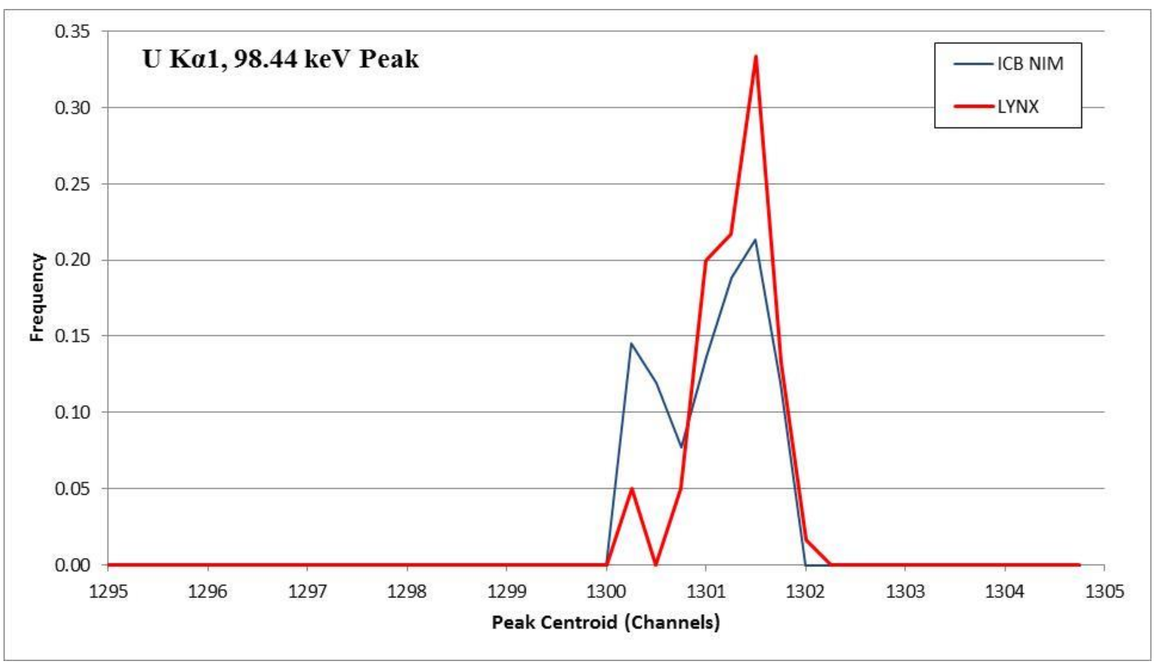

Figure 13. Frequency distribution for the observed 98.44 keV U $K_{\alpha 1,3}$ peak location for the ICB-NIM and LYNX XRF spectra as reported by the CHKED software.

4. Conclusions

The LYNX offer small but definite performance improvements relative to the ICB-NIM acquisition electronics for the HKED system. Use of the LYNX results in reduced dead-time losses translating to a typical 10% reduction in total measurement time (for equal live time settings). The single point energy stabilization offered by the LYNX was expected to be a source of bias in the HKED measurement, however (potentially due to a much more reliable baseline restorer) the LYNX and the ICB-NIM based acquisition systems provided essentially identical performance in terms of stability and detector resolution.

The LYNX offers single point energy stabilization while the ICB-NIM system allows 2-point energy stabilization. However, the observed differences in stability and peak resolution were small, amounting to no more than a few 10's of eV in peak location and width. It had been expected that without the option to stabilize on a low energy peak (e.g. the 22.1 keV Ag X-ray from ^{109}Cd decay) that the LYNX would not perform as well as the ICB-NIM. This may be because the Lynx's "baseline restoration" capability is more effective than anticipated or potentially due to the relatively clean mains power supplied to the HKED analog system. This could in principle be tested by injecting noise into the lines and comparing against the "clean" spectra.

Given the small differences in the observed stability and dead-time effects, it is not surprising that the choice of acquisition electronics had no statistically significant impact on the reported assay values. However, if the measurements were based on real time rather than live time acquisition, the LYNX modules would offer a slight gain in measurement precision due to the additional time available to acquire data.

Finally, although the observed performance of the KED detector channels indicates that gain stabilizer was in fact on during the measurements, as follow on to this work, we will re-visit the ambiguity of the gain stabilizer settings to provide a positive mechanism for determining the operational state of the stabilizer.

APPENDIX A. LYNX Settings for the HKED Measurements

		KED	XRF
MCA:	Type:	**Lynx**	**Lynx**
HVPS:	Type:	Internal	Internal
	Voltage:	-1500	-1000
	Overload Latch:	Disable	Disable
	Voltage Limit:	1500	1500
	Inhibit Latch:	Disable	Disable
	Inhibit Signal:	5V	5V
	Voltage Range:	-1500	-1500
	Output Polarity:	Neg	Neg
Digital Stabilizer	Type:	Internal	Internal
	Window	2	2
	Analog Range	0	0
	Analog Mode	Hold	Hold
	Stabilizer Centroid	10	1163
	Stabilizer Range	4	4
	Stabilizer Spacing	2	2
	Stabilizer Rate	0	0
	Correction Factor	0	6.56
	Event Multiplier	1	1
DSP Gain	Type:	Internal	Internal
	Coarse gain:	9.52E+00	1.13E+01
	Fine gain:	9.53E-01	9.27E-01
	S-fine gain:	1.00E+00	1.00E+00
	Amp gain:	1.00E+01	1.00E+01
	Conv. gain:	0	0
	Range	32768	32768
	Offset	0	0
	LLD	1.00E-01	1.00E-01
	Zero	0.00E+00	0.00E+00
	Fdisc. Mode	Auto	Auto
	Fdisc. Setting	1.00E+00	1.00E+00
	Inp. Polarity	1	1
	Inh. Polarity	0	0.00E+00
	LTC Mode	On	On
	Coinc. Mode	0	0
	PUR Guard	1.10E+00	1.10E+00
	Inhibit Mode	0	0
	LT Trim	500	500
	ICR	1.28E+03	1.44E+04
DSP Filter	Type:	Internal	Internal
	Rise Time	2.8	2.8
	Flat Top	0.6	0.6
	BLR mode	Auto	Auto
	Preamp type	RC	RC
	Pole zero	2362	2287

APPENDIX B. ICB-NIM Settings for the HKED Measurements

		KED	XRF
ADC:	Type:	**ICB 9635**	**ICB 9635**
	Mode:	PHA	PHA
	Peak Detect	Auto	Auto
	Coincidence Mode	Coinc	Coinc
	Coincidence Timing	Late	Late
	Transfer Timing	Overlap	Overlap
	Range:	2048	2048
	Offset:	0	0
	Conversion Gain	2048	2048
	LLD:	2	2
	ULD:	100.01	100.01
	Zero:	0	-0.08
Amplifier	Type:	**ICB 9615**	**ICB 9615**
	Shaping Mode	Gaussian	Gaussian
	BLR Mode	Sym	Sym
	LTC Mode	Normal	Normal
	Input Mode	Normal	Normal
	Input Polarity	Neg	Neg
	Inhibit Polarity	Pos	Pos
	Composite Gain	122.42	140.48
	Coarse Gain	50	100
	Fine Gain	2.45	1.4
	Superfine Gain	1	1
	Pole Zero Value	3014	2816
	Shaping Time	1 us	1 us
	Pileup Rejection	On	On
HVPS:	Type:	**ICB 9645**	**ICB 9645**
	Voltage	1495.6	997.07
	Voltage Limit	2000	1002.93
	Voltage Range	0	0
	Overload Latch	Disable	Disable
	Inhibit Latch	Enable	Enable
	Inhibit Signal	5V	5V
	Output Polarity	Neg	Neg
Gain Stabilizer:	Type:	**8233**	**8233**
	Zero Channel	246	292
	Gain Channel	978	1163